THE ASTROPHYSICAL JOURNAL, 556:847–857, 2001 August 1

THE $V-$EUV DELAY FOR DWARF NOVA OUTBURSTS: A CASE STUDY FOR VW HYDRI, U GEMINORUM, AND SS CYGNI

JOHN K. CANNIZZO
NASA/Goddard Space Flight Center, Laboratory for High Energy Astrophysics, Emergent Information Technologies, Inc., Code 662, Greenbelt, MD 20771; cannizzo@stars.gsfc.nasa.gov
Received 2000 November 16; accepted 2001 April 2

ABSTRACT

We present a parameter study using time-dependent calculations of the thermal limit cycle model for dwarf nova outbursts. Our goal is to delineate the dependence of the delay between the initial rapid rise of the visual and EUV fluxes during the start of an outburst on model parameters, concentrating on three bright nearby systems for which complete optical and EUV observations exist: VW Hydri, U Geminorum, and SS Cygni. For each system we compute 15 models spanning the early part of an outburst, taking the ratio of the instigation radius to the outer disk radius to be 0.5, 0.7, or 1.0 and adopting a value for the alpha viscosity parameter in the ionized disk of 0.1, 0.15, 0.2, 0.25, or 0.3. We confirm Smak's findings, which show a consistency of the standard model with observations. For these systems we infer that the outburst must be triggered at $\sim$0.7–0.8 of the outer disk radius to produce delays that are in accord with observations. We show that the level of EUV flux in outburst is dictated by the amount of material carried within the inward-moving heating front spike as it reaches the inner edge of the disk, and we reaffirm earlier work by Meyer et al. that found the heating front speed to be given by the alpha parameter times the sound speed within the heating spike. We also see a stagnation, or period of slow warming (first noted by Mineshige), during the early stages of thermal instability but find that it does not influence the $V-$EUV delay since it precedes the rapid rise in V at the start of the outburst. In studying the sensitivity of our results to the initial mass distribution, we find that if one decreases the surface density in the inner disk, interior to the instigation radius, the $V-$EUV delay can be lengthened by as much as a factor of 2. In addition, we find there to be a weak relation between the $V-$EUV delay and the value of the alpha viscosity parameter in quiescence.

Subject headings: accretion, accretion disks — binaries: close — stars: dwarf novae — stars: individual (SS Cygni, U Geminorum, VW Hydri)

1. INTRODUCTION

The accretion disk limit cycle model was proposed 20 years ago to account for the semiperiodic outbursts seen in dwarf novae (Meyer & Meyer-Hofmeister 1981). Dwarf novae are a subclass of cataclysmic variables (CVs), i.e., interacting binary stars in which a Roche lobe–filling K or M star transfers material through the inner Lagrangian point into an accretion disk about a white dwarf (WD) primary (Warner 1987, 1995). Dwarf novae are defined by their outbursts, which recur on intervals of between days and decades and have amplitudes of several magnitudes.

The limit cycle model posits that the rate of mass transfer into the outer part of the disk from the mass-losing star is constant on long timescales. (Actually, in the AM Her subclass of CVs, in which the WD is so strongly magnetized that no disk can form, one sees strong chaotic variations in the mass transfer rate from the secondary star [see Fig. 3 of Schreiber, Gänsicke, & Hessman 2000]. The mass-losing secondary stars in CVs should not differ between subclasses, so highly variable mass transfer should also be the rule in dwarf novae. For the nonmagnetic systems however, the accretion disk about the WD acts like a low-pass filter that responds only to slow variations, i.e., those occurring on timescales that are long compared to the viscous time in the outer disk of $\sim$1 yr.) The accretion disk limit cycle model is based on the theoretical finding that the steady state relation between effective temperature $T_{\rm eff}$ and surface density Σ at a given radius forms a hysteresis with two stable branches, one for ionized gas and one for neutral gas. When a series of steady state solutions for a given radius and varying rate of accretion $\dot{M}$ are plotted as $T_{\rm eff}$ versus Σ, one sees an S-shaped curve. The basic idea is that in the quiescent state of dwarf novae, matter is accumulating and the mass of the accretion disk is increasing. The mass flow within the disk is highly nonsteady, and the rate of removal of mass from the inner disk is many orders of magnitude below that at which it is being supplied at the outer edge. In the outburst state the opposite holds: the rate of mass removal from the inner disk onto the central accretor exceeds the rate of mass supply to the outer disk edge, which results in a decrease in disk mass. Thus, both the high- and low-state disks are unstable in the sense that they continually attempt to revert to the opposite state. For recent reviews see Osaki (1996) and Cannizzo (1993a, 1998c).

Following the initial vertical structure papers that established the physical underpinnings for the limit cycle idea (Meyer & Meyer-Hofmeister 1981, 1983; Cannizzo, Ghosh, & Wheeler 1982; Cannizzo & Wheeler 1984; Smak 1984; Faulkner, Lin, & Papaloizou 1983; Mineshige & Osaki 1983), authors began to explore detailed aspects of the model using time-dependent codes (Papaloizou, Faulkner, & Lin 1983; Lin, Papaloizou, & Faulkner 1985; Smak 1984; Meyer & Meyer-Hofmeister 1984; Mineshige & Osaki 1985; Cannizzo, Wheeler, & Polidan 1986, hereafter CWP; Cannizzo & Kenyon 1987, hereafter CK; Pringle, Verbunt, & Wade 1986, hereafter PVW). More recent time-dependent work has concentrated on the development of increasingly sophisticated numerical models that are utilized to study different systematic effects inherent in the

calculations (e.g., Mineshige 1988; Ichikawa & Osaki 1992, 1994; Cannizzo 1993b, hereafter C93b, 1994; Ludwig, Meyer-Hofmeister, & Ritter 1994; Ludwig & Meyer 1998; Hameury et al. 1998; Menou, Hameury, & Stehle 1999; Truss et al. 2000; Buat-Meńard, Hameury, & Lasota 2001, hereafter BHL). These later studies represent an advancement over the earlier ones, but some of the difficulties in reconciling theory with observation remain. For instance, BHL present global time-dependent computations (using the model described in Hameury et al. 1998) that include the effects of heat input due to the stream-disk impact and tidal torque. They show that such models produce sequences of alternating long and short outbursts, triggered at large radii with similar peak luminosities, thereby rectifying some of the difficulties evident in the computations of C93b. Figure 7 of BHL shows a change in sequencing from all short to all long outbursts as the secondary mass transfer rate $\dot{M}_T$ is made to increase, while their Figure 4 shows a decrease in the interoutburst quiescent intervals with increasing $\dot{M}_T$. Combining these results gives a prediction that $\langle N(L)/N(S)\rangle$, the moving long-term average of the ratio of long to short outbursts in a long time series (during which there are variations in $\dot{M}_T$) should be anticorrelated with $\langle t_q\rangle$, the moving long-term average of the quiescent interval. In other words, if long-term variations in $\langle \dot{M}_T\rangle$ occur and affect the outbursts, then during times when $\langle \dot{M}_T\rangle$ is larger and therefore more long outbursts are occurring, the quiescent intervals should be shorter. The long-term light curve of SS Cyg shows the opposite: a strong positive correlation between $\langle N(L)/N(S)\rangle$ and $\langle t_q\rangle$ (see Figs. 14 and 15 of C93b).

One observation of interest is the delay between the rise of the optical and EUV fluxes in the so-called fast-rise outbursts that are seen in several dwarf novae. For these systems one sees the optical begin to rise about 1 day before the EUV. This is accounted for in the model by the fact that the optical flux, which is weighted basically by the emitting area of the disk, arises predominantly at large radii, while the EUV flux comes from small radii close to the WD (Cannizzo 1996, 1998a). Therefore, the delay represents the time for the heating transition wave that communicates the onset of thermal instability to travel from large radii where the instability begins down to the WD. The earliest studies exploring the $V-$EUV delay found a basic consistency between theory and observation (Smak 1984; CWP), while later authors found an apparent discrepancy (PVW; CK). Mineshige (1988) presents a detailed time-dependent study of the rise to outburst using more sophisticated input physics than some of the earlier authors. In particular, he uses physically realistic values of the specific heat as a function of density and temperature, $c_P(\rho, T)$, and finds a "stagnation" stage in the early phase of the outburst during which the disk midplane temperature is stalled at $\sim 10^4$ K because of the large c_P. Some other aspects of his model rely on detailed $T_{\rm eff}(\Sigma)$ features near the local maximum in surface density $\Sigma_{\rm max}$ that depend strongly on specifics of the vertical structure calculations.

Smak (1998) presents a thorough investigation of the problem and traces the failure of the later authors to their inability to produce outbursts that begin at sufficiently large radii. The reason this is critical is at least partly due to the fact that outbursts that begin too close to the inner edge, referred to as "inside-out" outbursts (CWP) or "type B" outbursts (Smak 1984), have a fundamentally different shape than outbursts that begin at large radii, referred to as "outside-in" outbursts (CWP) or "type A" outbursts (Smak 1984). Basically, type A outbursts have a fast rise and type B outbursts have a slow rise. The difference has to do with the rate of enhancement of surface density in the inner disk during the early stage of the outbursts (see CWP for an explanation). Furthermore, the dividing line between these two types of outbursts is quite sharp; for a triggering or instigation radius $r_{\rm instig}$ that is less than some critical radius $r_{\rm crit}$, one obtains type B outbursts, whereas for $r_{\rm instig} > r_{\rm crit}$, type A outbursts occur (see Fig. 6b of Cannizzo 1998b). In summary, in order to obtain the needed delay, one requires an outburst that triggers at a sufficiently large radius, so that not only is the outburst type A, but also the time for the heating front to travel to the inner disk edge $\int dr\,|v_F|^{-1}$ is long enough to equal the observed $\Delta t(V-{\rm EUV})$.

Smak (1998) shows that the flux distributions utilized in the calculations of the V and EUV fluxes (i.e., Planckian vs. stellar or Kurucz type) are of secondary importance, in contrast to what might be inferred from some reviews (e.g., Cannizzo 1993a, 1998c). This is particularly true in comparing the V and EUV fluxes; in fact, for the latter we may simply use $\dot{M}_{\rm inner}$, the rate of mass loss from the inner disk onto the WD, as a tracer of the EUV flux. In this regard, the *Extreme Ultraviolet Explorer* satellite (*EUVE*) is an ideal instrument for studying accretion onto WDs: the peak in its response function lies at $\lambda \simeq 100$ Å, or $E \simeq 0.1$ keV, and the effective temperature in the disk is

$$T_{\rm eff} = T_*\left(\frac{r_{\rm WD}}{r}\right)^{-3/4}\left[1-\left(\frac{r_{\rm WD}}{r}\right)^{1/2}\right]^{1/4}, \qquad (1)$$

where $\sigma T_*^4 = (3/8\pi)(GM_{\rm WD}/r_{\rm WD}^3)\dot{M}$ (Shakura & Sunyaev 1973). Evaluating gives

$$T_* = 18.7\ {\rm eV}\left(\frac{\dot{M}}{10^{18}\ {\rm g\ s^{-1}}}\right)^{1/4}\left(\frac{M_{\rm WD}}{1\ M_\odot}\right)^{1/4} \times\left(\frac{r_{\rm WD}}{5\times 10^8\ {\rm cm}}\right)^{-3/4}. \qquad (2)$$

The maximum temperature in the accretion disk [evaluated at $(49/36)r_{\rm WD}$] is

$$0.488T_* = 9.1\ {\rm eV}\left(\frac{\dot{M}}{10^{18}\ {\rm g\ s^{-1}}}\right)^{1/4}\left(\frac{M_{\rm WD}}{1\ M_\odot}\right)^{1/4} \times\left(\frac{r_{\rm WD}}{5\times 10^8\ {\rm cm}}\right)^{-3/4}. \qquad (3)$$

Therefore the peak in the accretion disk spectrum occurs at about a factor of 10 lower in energy than the *EUVE* response peak. This region of the spectrum is largely masked by interstellar absorption. The flux seen by *EUVE* for dwarf novae in outburst must be predominantly coming from the boundary layer around the WD. We idealize this flux as representing the mass flux directly onto the WD from the inner edge of the accretion disk.

The perception of a "UV delay problem" led many authors to consider scenarios for the quiescent evolution of dwarf novae in which the surface density is eroded at small radii via some type of low-level accretion onto the WD such that a hole is created in the inner disk, thereby forcing the outbursts to be triggered at larger radii than they would have otherwise (e.g., Livio & Pringle 1992; King 1997;

Stehle & King 1999; Hameury, Lasota, & Dubus 1999). Although this specific impetus for such models is rendered invalid by Smak's study, there may be other reasons to invoke some quiescent evaporation of the disk in dwarf novae such as the observations of significant X-ray flux coming from the central star in quiescence, which cannot be explained in the standard model (e.g., Mukai et al. 1997; van Teeseling 1997; Pratt et al. 1999).

In this work we expand on Smak's (1998) investigation by carrying out a detailed parameter study for three specific systems using a time-dependent model for the development of the onset and subsequent evolution of the accretion disk following the start of a dwarf nova outburst. We use parameters appropriate for VW Hydri, U Geminorum, and SS Cygni because for these dwarf novae there exist simultaneous V and EUV data during outburst (Mauche, Mattei, & Bateson 2001, hereafter MMB). The V data in MMB were obtained by the American Association of Variable Star Observers (AAVSO) and the Variable Star Section/Royal Astronomical Society of New Zealand (VSS/RASNZ); their EUV data comes from *EUVE*. We perform a parameter study over $\alpha_{\rm hot}$, the viscosity parameter characterizing the hot state of the disk, and $r_{\rm instig}/r_{\rm disk}$, the ratio of the triggering radius for thermal instability to the outer disk radius. We also examine the sensitivity of the results to the initial mass profile in the disk. Specifically, we examine (1) the effect of putting all the initial mass into a torus at $r_{\rm instig}$ and leaving only a small surrounding background surface density $\Sigma_{\rm floor}$ and (2) the effect of varying $\alpha_{\rm cold}$, which governs the quiescent disk mass.

2. MODEL CALCULATIONS

2.1. *Numerical Model*

We utilize a new version of our standard time-dependent disk instability code, recently rewritten from FORTRAN into C++. The code has been tested to ensure numerical stability. The time-dependent equations that we solve are given in C93b. One combines the mass and angular momentum conservation equations into a diffusion equation for surface density, written under the assumptions of Keplerian rotation $v_\phi(r) = (GM_{\rm WD}\, r^{-1})^{1/2}$ and cylindrical symmetry. One similarly writes an energy equation under the assumption of cylindrical symmetry. Together these two coupled nonlinear differential equations provide a means for calculating small changes in the surface density $\delta\Sigma(r, t)$ and midplane temperature $\delta T(r, t)$ for a given physical state of the disk specified by $\Sigma(r, t)$ and $T(r, t)$.

If the disk is entirely on either the lower or upper stable branch of solutions (i.e., completely neutral gas or completely ionized gas), then only the diffusion equation for $\Sigma(r, t)$ is solved in that time step. For such solutions we utilize the power-law scalings for $T(\Sigma, r, \alpha)$ given in C93b to determine the midplane temperature. For radii in which thermal transitions are occurring, we must also solve the energy equation, which contains both direct heating and cooling terms characterizing the departure from thermal equilibrium in a given annulus as well as terms involving advection (the physical transport of heat by the flow) and terms representing the radial energy flux within the body of the disk. As in C93b, we interpolate α logarithmically between $\alpha_{\rm cold}$ and $\alpha_{\rm hot}$, based on the local value of T compared to $T(\Sigma_{\rm min})$ and $T(\Sigma_{\rm max})$. The advective terms contain the local flow velocity $v_r = -(3\nu/r)[\partial \log (\nu\Sigma r^{1/2})]/\partial \log r$, which is calculated through (upstream) differencing at each grid point. Two terms contribute to the radial flux of energy, a viscous term $J_V = \frac{3}{2}(c_P\, \nu\Sigma/r)\partial(r\partial T/\partial r)/\partial r$ (introduced by Mineshige 1986) and a radiative term $J_R = -h/r[\partial(rF_r)/\partial r]$, where $F_r = -[4acT^3/(3\kappa\rho)]\partial T/\partial r$ (introduced by Faulkner et al. 1983). In C93b, the radiative term J_R was not utilized because of problems with numerical stability. In this work we have included this term, using the analytical scalings for the opacity κ given in Lin & Papaloizou (1985). As we shall see later, $|J_R/J_V| \ll 1$ in general, which is ironic given that the introduction of J_R preceded that of J_V.

We take $N = 1000$ grid points equally spaced in $\sqrt{r}$ between $r_{\rm WD}$ and $r_{\rm disk}$. For the inner disk radius $r_{\rm WD}$, we use the analytical white dwarf radius-mass scaling of B. Paczyński, as given by Anderson (1988, see his eq. [33]). We specify an initial surface density profile so as to force the triggering for outburst at a given radius. This is accomplished by starting with a Gaussian profile for $\Sigma(r)$ centered at some r_c that is 0.5, 0.7, or 1.0 times the outer disk radius $r_{\rm disk}$. We set the FWHM of the Gaussian at $0.03r_c$ and take $\Sigma(r_c) > \Sigma_{\rm max}(r_c)$. Thus we idealize the $t = 0$ state of the disk to consist of two components: a narrow torus representing material added from the secondary and a broad component ($0.3\Sigma_{\rm max}$) representing material left from the previous outburst. In view of the concerns raised by Gammie & Menou (1998), we consider the assumption of a constant and uniform $\alpha_{\rm cold}$ to describe the quiescent evolution as suspect, and therefore we do not run complete cycles as in Smak (1998). Gammie & Menou point out that the large resistivity of the neutral gas expected in quiescence may hamper the efficiency of the magnetorotational instability (MRI), the currently favored mechanism for angular momentum transport in accretion disks (Balbus & Hawley 1991; Hawley & Balbus 1991; for a review see Balbus & Hawley 1998). Unfortunately there is no quantitative way at the present time to carry out full time-dependent calculations based on a physically self-consistent formalism that satisfies Gammie & Menou (although Menou 2000 presents a step in this direction). We must assume the existence of an $\alpha_{\rm cold}$ ($=0.02$) so as to set the critical scalings associated with $\Sigma_{\rm max}$. We examine five values of $\alpha_{\rm hot}$: 0.1, 0.15, 0.2, 0.25, and 0.3. We consider three specific systems and so adopt values of the central mass $M_{\rm WD}$ and outer disk radius $r_{\rm disk}$ relevant to each. The systemic values taken for VW Hyi, U Gem, and SS Cyg models are $(M_{\rm WD}/M_\odot,\ r_{\rm disk}/10^{10}\ {\rm cm}) = (0.63, 2.26)$, $(1.26, 4.54)$, and $(1.19, 5.86)$, respectively. These values come from $M_{\rm WD}$ and $P_{\rm orbital}$ values in Ritter & Kolb (1998), where we take $r_{\rm disk} = 0.9r(L_1)$. Therefore we carry out a total of 45 runs: five $\alpha_{\rm hot}$ values times three $r_{\rm instig}/r_{\rm disk}$ values times three systemic parameter values. For each run, we compute the absolute visual magnitude M_V, the rate of mass flow within the inward-moving heating front, and the local rate of mass flow at $1.1r_{\rm WD}$, which we take to be the rate of accretion onto the WD. This is used as a tracer of the EUV flux.

2.2. *Long-Term Light Curves*

Figure 1 shows the results of our 45 trials. The three panels correspond to VW Hyi, U Gem, and SS Cyg, respectively. The delay $\Delta t(V-{\rm EUV})$ is measured between the onset of the rapid rise in V and the increase in $\dot{M}$ onto the WD. We define the onset of the rapid increase in V flux by a small spike in V that accompanies the end of the stagnation stage. The horizontal dashed lines in each panel show the

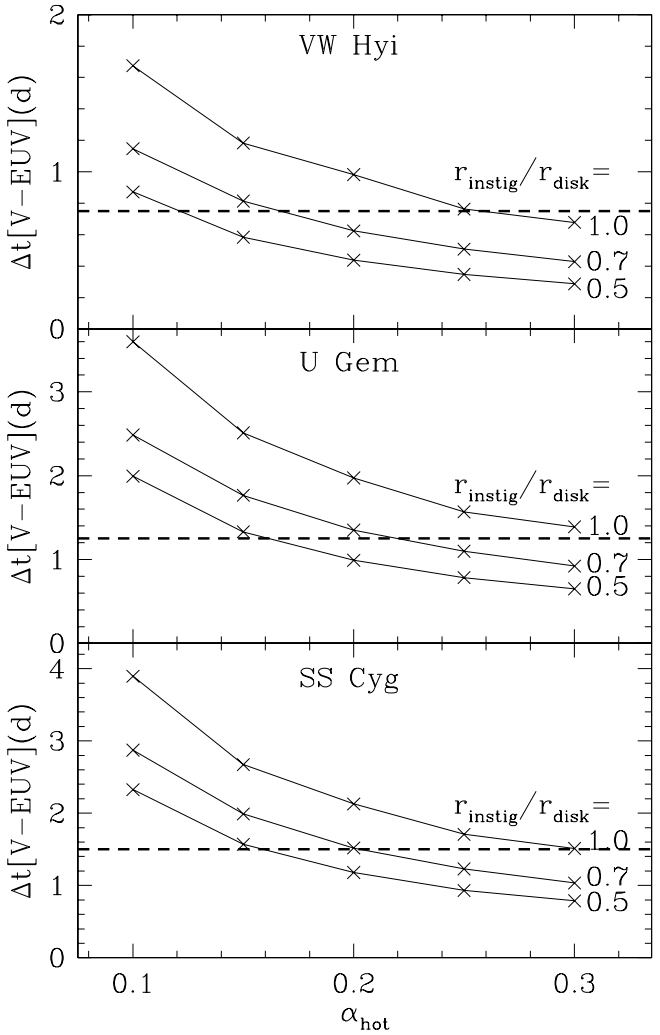

FIG. 1.—Delay between the initial rapid rise in V and EUV for our trials, which model VW Hyi (*top panel*), U Gem (*middle panel*), and SS Cyg (*bottom panel*). Each panel contains the results from 15 trials, spanning a range of five values of $\alpha_{\rm hot}$ and three values of $r_{\rm instig}/r_{\rm disk}$. The values of the central masses are taken to be 0.63, 1.26, and 1.19 $M_\odot$, respectively, and the disk outer radii $r_{\rm disk}$ are 2.26×10^{10}, 4.54×10^{10}, and 5.86×10^{10} cm, respectively (Ritter & Kolb 1998). *Horizontal dashed lines*: The observed delay as inferred from observations.

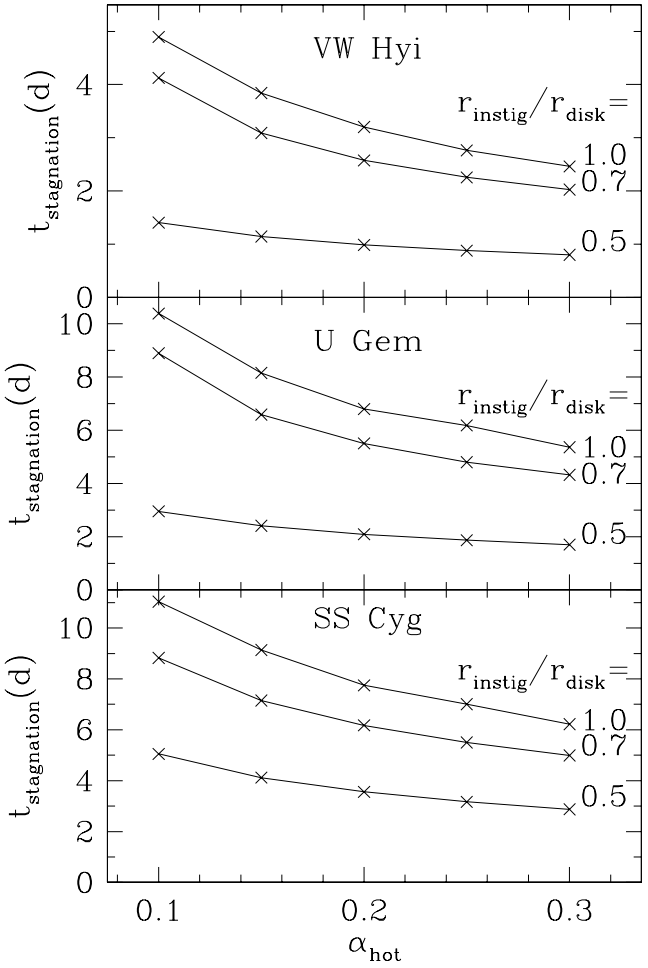

FIG. 2.—Durations of the stagnation period of slow heating that precedes the rapid rise in the V flux for the simulations shown in Fig. 1. The nonlinear dependence of $t_{\rm stagnation}$ on $r_{\rm instig}/r_{\rm disk}$ stems from the density dependence of the maximum in the specific heat c_P on density.

observed delay between the rapid rises in V (from AAVSO and VSS/RASNZ observations) and EUV (from *EUVE* observations), taken from MMB. The delays are 0.75 days for VW Hyi, 1.25 days for U Gem, and 1.5 days for SS Cyg. Our computed delay does not scale exactly linearly with $r_{\rm instig}/r_{\rm disk}$ because the effective start of strong heating that follows stagnation comes after a period of slow growth of the thermally unstable annulus. Thus after stagnation ends, one is left with a hot annulus that is fairly broad, so its inner edge lies somewhat interior to $r_{\rm instig}$. This instant of time marks the onset of the rapid rise in V and the launching of the heating front. Figure 2 shows the duration of the stagnation intervals for the trials in Figure 1. These times are generally longer than the $V-$EUV delay time intervals that immediately follow them.

Figure 3 shows the outburst onset for our best-fit SS Cyg model, for which $\alpha_{\rm hot} = 0.2$ and $r_{\rm instig}/r_{\rm disk} = 0.7$. (Our preference for $\alpha_{\rm hot} = 0.2$ comes from Smak's 1999 investigation of the Bailey relation [Bailey 1975] between outburst decay rate in V and orbital period for dwarf nova outbursts.) One sees a long stagnation stage caused by the increased specific heat of gas at $\sim 10^4$ K. Physically, the addition or subtraction of heat goes predominantly into changing the degree of partial ionization of the gas; the resultant temperature change is minimal. There is a spike in V at $t \simeq 6.1$ days accompanying the end of stagnation. The lower panel shows the local rate of mass flow associated with the inward-moving heating front on the same scale as that within the disk at $1.1 r_{\rm WD}$. We calculate this by evaluating $\dot{M}(r) = 2\pi r \Sigma v_r$ at the local maximum in $\Sigma(r)$, which defines the heating front. This flow rate peaks at $\sim 10^{20}$ g s^{-1}, just after the onset of the front propagation. Although this represents an enormous local rate of accretion, it may have negligible observational consequences owing to the shallow gravitational potential at large radii. It is informative to plot $\dot{M}_{\rm front}$ and $\dot{M}_{\rm WD}$ on the same scale so one can see the causal relationship between the two; the rapid rise in $\dot{M}_{\rm WD}$ after the heating front reaches the inner edge is a consequence of the arrival of material carried within the heating spike at the WD. The amplitude of $\dot{M}_{\rm WD}$ is determined by the mass carried in the heating front spike, and the subsequent slower rise to maximum over the next ~ 0.3 days is determined by the sloshing action of gas as the outburst density profile $\Sigma(r) \propto r^{-3/4}$ is established.

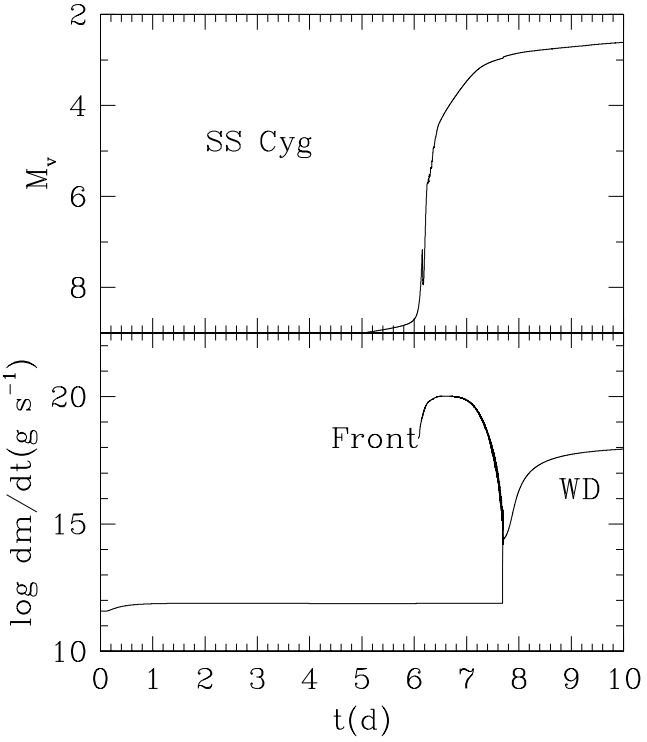

FIG. 3.—A detailed view of our SS Cyg model taken from the center of the grid of models shown in the bottom panel of Fig. 1, for which $\alpha_{\rm hot} = 0.2$ and $r_{\rm instig}/r_{\rm disk} = 0.7$. Shown are the absolute visual magnitude M_V vs. time (*top panel*) and two curves giving the local mass flow rate $2\pi r\Sigma(r)v_r(r)$, one evaluated at the peak of the inward-moving heating spike and one at $1.1r_{\rm WD}$, where $r_{\rm WD} = R(M_{\rm WD}) = 4.2 \times 10^8$ cm for $M_{\rm WD} = 1.19\ M_\odot$.

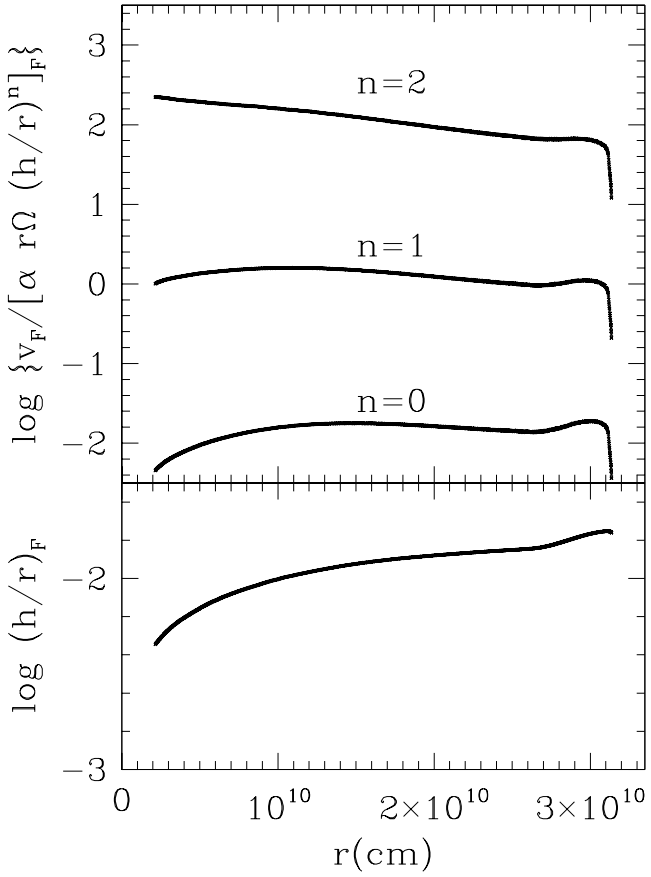

FIG. 4.—Evolution of the heating front speed v_F (*top panel*) and h/r (*bottom panel*) evaluated within the heating front, for the model shown in Fig. 3, normalized to $\alpha r\Omega(h/r)^n$, evaluated at the local maximum in the heating front. The best fit to v_F is $\alpha r\Omega(h/r) = \alpha c_S$ (i.e., that for which the exponent $n = 1$).

Figure 4 shows the speed of the heating front and the h/r values within the heating front for the model from Figure 3. The top panel shows the speed in units of $\alpha r\Omega(h/r)^n$, where all quantities are evaluated at the local maximum in Σ within the heating front and n is taken to be 0, 1, or 2. The front speed closely follows $\alpha r\Omega(h/r)^1$, or αc_S (local hydrostatic equilibrium gives $c_S = \Omega h$), confirming previous work by Meyer (1984) and Lin et al. (1985). Equation (1) of Smak (1998) gives a scaling for the "radial velocity of the accreting matter," which would correspond to our $n = 2$ case. We can exclude this expression as being the heating front speed. It is representative, however, of the general viscous flow speed of gas within the parts of the disk that are far from the front (see Fig. 2 of Cannizzo 1998b). Figure 5 shows the front speed and corresponding values of h/r within the front in the SS Cyg models for which $r_{\rm instig}/r_{\rm disk} = 0.7$. The evolution of h/r is virtually identical for all five curves, so the heating front speed just scales linearly with α.

Figure 6 shows the evolution of $\Sigma(r, t)$ and $T(r, t)$ for the same model shown in the previous figures. Each line is separated by 0.25 days. Three distinct phases are evident. (1) The first $\sim$6 days of evolution encompass a slow shift from the initial profile. The initial torus at 4×10^{10} cm smears and the temperature increases slowly. It is this period of evolution for which Mineshige (1988) coined the term "stagnation." Stagnation is a consequence of the increase in the specific heat by a factor of $\sim$10–50 for gas at $\sim 10^4$ K (see Fig. 1 of C93b). (2) After stagnation has ended, a strong spike in $\Sigma(r)$ develops at the inner edge of the annular heating region, and the spike moves to smaller radii. The amplitude of the spike decreases strongly with decreasing radius, approaching zero as $r_{\rm front} \rightarrow r_{\rm WD}$. This stage lasts 1.5 days and is the cause of the $V-$EUV delay; this is the time required for the effect of strong heating (i.e., poststagnation) to be communicated to the inner edge of the disk. (3) Now the entire disk has made the transition from neutral to ionized gas, but the flow pattern $\dot{M}(r)$, although by now altered significantly from the quiescent profile, is still out of steady state. During the rest of the evolution, the $\Sigma(r)$ distribution changes in the sense that material at large radii shifts to smaller radii, asymptotically approaching $\Sigma(r) \propto r^{-3/4}$ and $\dot{M}(r) \simeq$ constant.

Figure 7 shows the evolution of the ratios of several terms in the energy equation to the heating term during stagnation. Specifically, we follow $|C/H|$, $|J_V/H|$, and $|J_R/H|$, where H is the heating term $\frac{9}{8}\nu\Omega^2\Sigma$, C is the cooling term $\sigma T_{\rm eff}^4$, and J_V and J_R are the viscous and radiative radial flux terms given earlier. One can see the increase with time of the annular extent of the thermally unstable ring. Heating initially exceeds cooling by a factor of $\sim$3 at the center of the annulus. The viscous term J_V is comparable to C, although $|J_V/H|$ is more nearly constant with radius. By comparing the second and third panels, one sees the insignificance of the radiative term compared to the viscous term. The relative importance of these two terms has not been previously presented in a quantitative way, although some authors have commented that J_R is small (e.g., Ludwig & Meyer 1998). Figure 8 shows the evolution of the

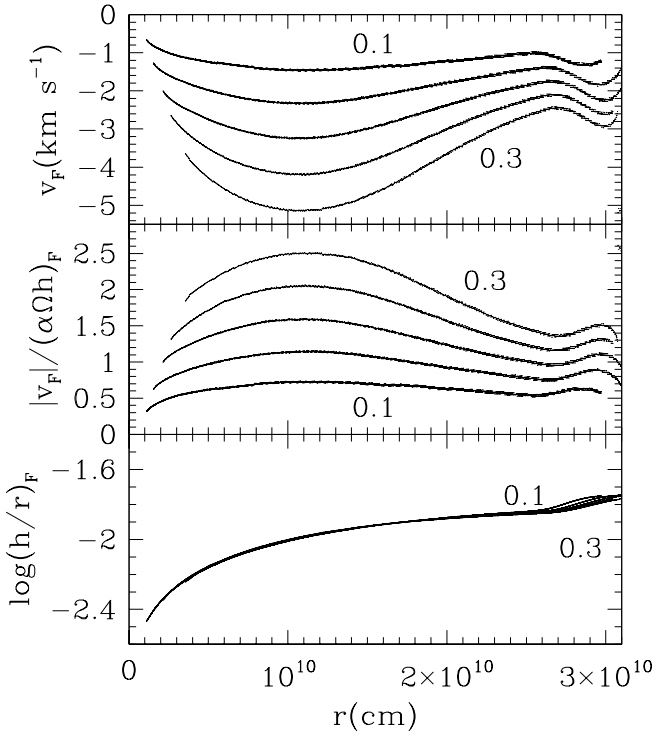

FIG. 5.—Evolution of the heating front speed v_F in km s^{-1} (*top panel*), normalized to $\alpha\Omega h$, evaluated at the local maximum in the heating front (*middle panel*); h/r (*bottom panel*), also evaluated at the local maximum within the heating front for the SS Cyg models, for which $r_{\rm instig}/r_{\rm disk} = 0.7$. Five curves shown are for $\alpha_{\rm hot} = 0.1$, 0.15, 0.2, 0.25, and 0.3, with the larger $\alpha_{\rm hot}$ values corresponding to larger $|v_F|$ values. The middle panel shows an increasing deviation in $|v_F|$ from αc_S as $\alpha_{\rm hot}$ increases. The value of h/r within the heating front is nearly independent of $\alpha_{\rm hot}$.

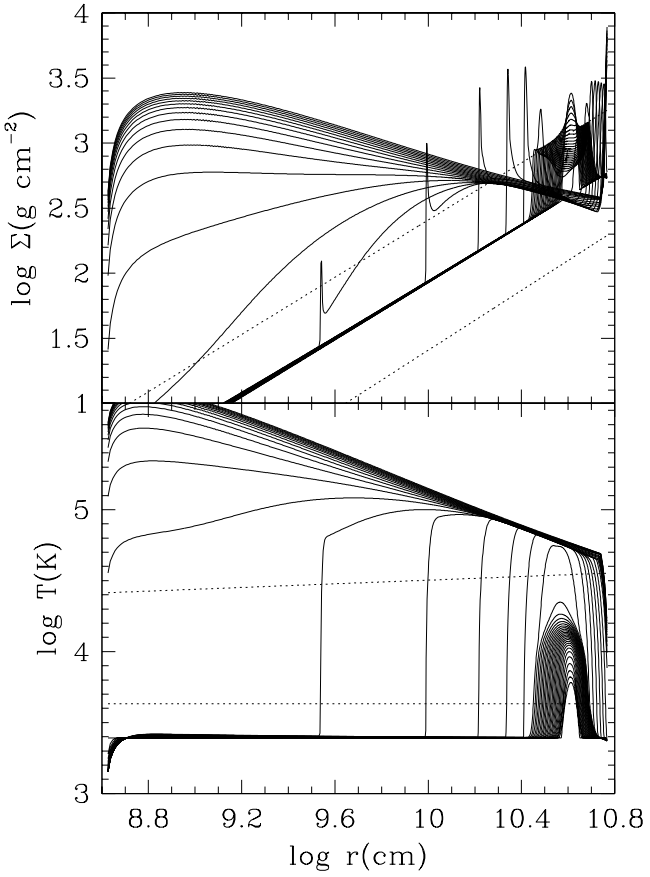

FIG. 6.—Evolution of surface density $\Sigma(r, t)$ and midplane temperature $T(r, t)$ over 12 days for the model shown in Fig. 3. The initial profile is a Gaussian in $\Sigma(r)$ centered at $r_c \simeq 4 \times 10^{10}$ cm. Each curve is separated by 0.25 days. The three stages evident in the evolution are (1) a stagnation stage (spanning $\sim$6 days or $\sim$25 curves) during which the initial profile broadens by a factor of $\sim$2–3, and $T(r_c) \simeq 10^4$ K; (2) a subsequent period of more rapid evolution in which a strong spike in Σ develops and propagates inward (spanning $\sim$1.5 days or 5–6 curves); and (3) a period of readjustment in $\Sigma(r)$ during which Σ at smaller radii is built up as the disk makes a transition from being highly out of steady state [i.e., $\dot{M}(r) \neq$ const] to quasi-steady state [i.e., $\dot{M}(r) \simeq$ const], in which Σ varies roughly as $r^{-3/4}$.

terms in the thermal energy equation $\Delta T = \Delta t$(term 1 − term 2 − term 3), where the direct heating and cooling term is term 1 $= 2(H - C + J)/(c_p \Sigma)$, the PdV work term is term 2 $= \Re T/(\mu c_p)(1/r)\partial(r v_r)/\partial r$, and the advective term is term 3 $= v_r \partial T/\partial r$ (C93b). The PdV term is less than term 1 by about an order of magnitude, while the advective term is comparable to term 1 in the interior of the stagnation annulus and exceeds it slightly near the edges.

2.3. *Sensitivity to the Initial Mass Distribution*

The calculations of § 2.4 are based on simplifying assumptions adopted for generality that the initial mass distribution in the accretion disk at the time of triggering is a sum of two distributions: a broad one, $\Sigma_{\rm broad}$, representing matter left over from the previous outburst, and a narrow one, $\Sigma_{\rm narrow}$, representing matter transferred from the secondary star, which accumulates over some annular extent between the specific angular momentum radius and the outer disk edge. As discussed previously, given the uncertainty about the physical processes that operate during quiescence and influence the $\Sigma(r)$ evolution, our parameter study is intended to explore a broader range of triggering conditions than might be obtained in previous studies such as that of Smak (1998), which follow the evolution of the accretion disk through several complete cycles under the assumption of some $\alpha_{\rm cold}$ that is constant in space and time.

We now look at the sensitivity of our results to the initial mass distribution. The $V-$EUV delay essentially represents the time for the heating front to traverse the disk from $r_{\rm instig}$ to $r_{\rm WD}$; therefore we need to understand how v_F depends on the background $\Sigma(r)$ profile. To explore this we now impose the additional constraint on our models that $\Sigma_{\rm broad}(r) \leq \Sigma_{\rm floor}(r)$, where in separate runs we take $\Sigma_{\rm floor}$ to be 0.01, 0.1, 1, 10, or 100 g cm^{-2}. We limit the maximum value of $\Sigma_{\rm broad}(r)$ to $0.7\Sigma_{\rm max}(r)$. Figure 9 shows the results for our SS Cyg model, in which $\alpha_{\rm cold} = 0.02$ and $\alpha_{\rm hot} = 0.2$. The dashed lines indicate the delays from our previous models. One can see that as $\Sigma_{\rm floor} \rightarrow 0$, the time delays asymptote to a constant value equal to roughly twice that found earlier in the results for which $\Sigma_{\rm broad} = 0.3\Sigma_{\rm max}$. In our idealization of a background mass distribution plus a narrow torus, this limiting case corresponds to that in which all the disk mass is initially contained in the torus. One might have possibly expected the heating front to die out as $\Sigma_{\rm floor} \rightarrow 0$; we can definitely exclude this. The strong gradient in viscous stress within the expanding hot region is the primary agent that determines the properties of the heating front; the background medium into which the hot material expands affects the expansion rate only to second order, given that the viscous stresses therein are much smaller. Once $\Sigma_{\rm floor}$ drops below $\sim$1 g cm^{-2}, $(v\Sigma)_{\rm floor} \ll (v\Sigma)_{\rm front}$, so the background

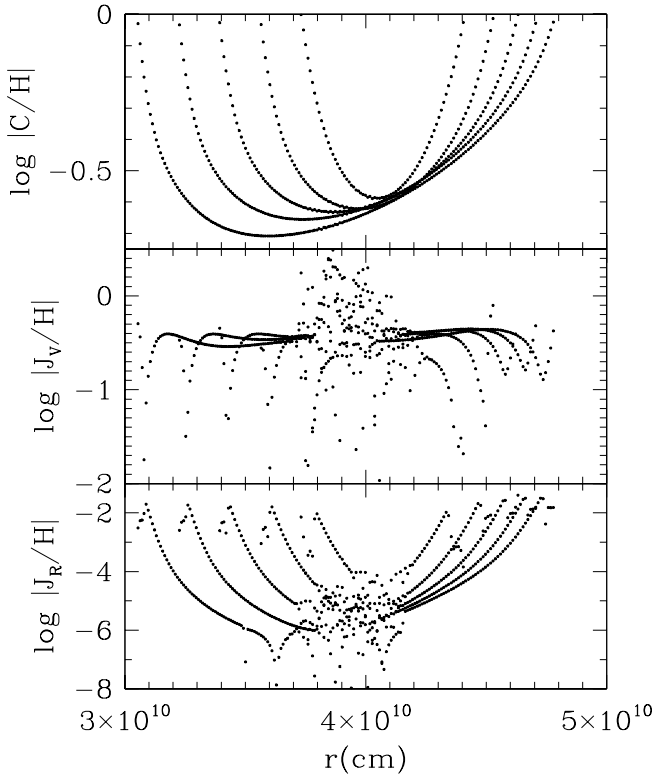

FIG. 7.—Evolution of different terms in the energy equation with respect to the heating term for the model shown in Fig. 3. The curves represent the state of the disk at $t(d) = 1$, 2, 3, 4, and 5, which covers the stagnation period. Shown are the logarithms of the absolute values of the ratios of (1) the cooling term C to the heating term H (*upper panel*), (2) the viscous radial flux term J_V to H (*middle panel*), and (3) the radiative radial flux term J_R to H (*lower panel*). The annular extent of thermal instability increases with time.

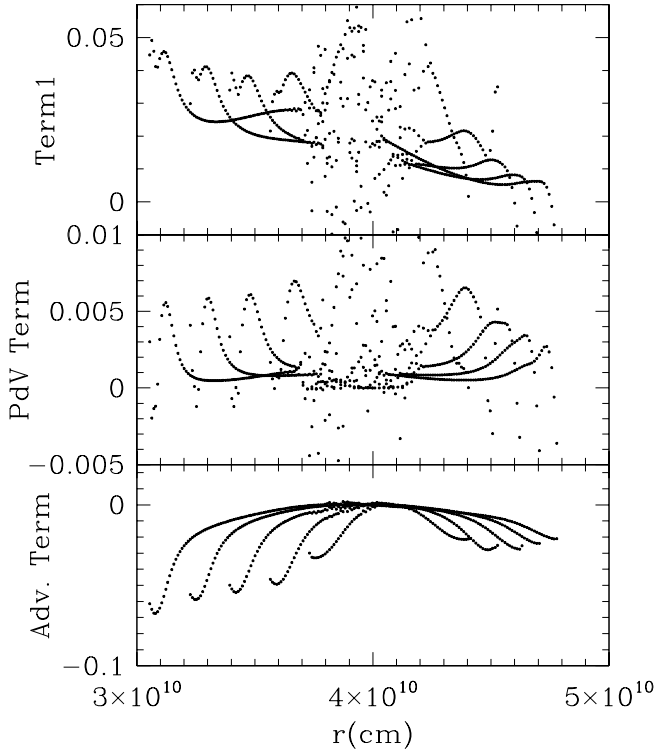

FIG. 8.—Evolution of the three terms in the energy equation for the same time steps as in Fig. 7. Shown are the terms characterizing the direct, local heating and cooling $2(H - C + J)/(c_p\Sigma)$ (*upper panel*), the PdV work term $\Re T/(\mu c_p)(1/r)\partial(rv_r)/\partial r$ (*middle panel*), and the advective term $v_r\,\partial T/\partial r$ (*lower panel*). The temperature change in a given time step $\Delta T = \Delta t$ (term 1 − term 2 − term 3), where Δt is the time step. The PdV term is less than term 1 by about an order of magnitude, while the advective term is comparable to or larger than term 1.

profile does not influence v_F. Figure 10 shows the evolution of v_F for the runs accompanying Figure 9. The trials for $\Sigma_{\rm floor} = 0.01$, 0.1, and 1 g cm^{-2} are indistinguishable. For larger $\Sigma_{\rm floor}$, the heating front speed $|v_F|$ increases because the greater disk mass supports a larger $\Sigma_{\rm front}$ and therefore larger value of $(h/r)_{\rm front}$.

Finally, we look at the effect of varying $\alpha_{\rm cold}$ by a factor of 2 around our nominal value of 0.02. The critical surface density $\Sigma_{\rm max}$ scales as $\alpha_{\rm cold}^{-0.8}$; therefore larger $\alpha_{\rm cold}$ values translate into smaller accretion disk masses, which would lead one to predict smaller amplitude heating spikes traveling at slower speeds. Figure 11 indeed shows that the delays are longer for larger $\alpha_{\rm cold}$; however, the dependence is weak: a factor of 4 increase in $\alpha_{\rm cold}$ only increases the front travel time $\Delta t(V-{\rm EUV}) = \int dr\,|v_F|^{-1}$ by $\sim$10%–20%. Figure 12 shows the variation in the front speed v_F. The maximum variation in $|v_F|$ occurs at $\sim 10^{10}$ cm in these models, ranging from $\sim$3.6 to $\sim$2.5 km s^{-1} as $\alpha_{\rm cold}$ varies from 0.01 to 0.04. The variation at larger radii is smaller, which accounts for the relatively small range in $\Delta t(V-{\rm EUV})$ as a function of $\alpha_{\rm cold}$.

2.4. *Comparison with Menou, Hameury, & Stehle (1999)*

The most detailed and comprehensive study to date that investigates the structure and properties of transition fronts in accretion disks is that of Menou et al. (1999, hereafter MHS). These authors utilize a fully implicit adaptive mesh code (Hameury et al. 1998) with 800 radial grid points. Their dynamic allocation of grid points is optimized to place more grid points in regions with steep gradients. This offers a distinct advantage over a spatially fixed grid: their transition fronts generally contain $\sim$100 grid points and hence are well resolved even at small radii. Insofar as detailed comparisons can be made between our two studies, the results appear to be consistent. For example, in their presentation of results for "outside-in" heating fronts (see their §§ 3.2 and 3.3), which contain runs covering a variety of assumptions for $\alpha_{\rm cold}$ and $\alpha_{\rm hot}$, they find $|v_F|$ values of several km s^{-1}, as do we. In their discussion they comment that $|v_F| \propto \alpha_{\rm hot}$, consistent with our results shown in Figure 5. The front speeds depicted in MHS are only shown in units of km s^{-1}; therefore one cannot quantitatively assess their departures of $|v_F|$ from $(\alpha c_S)_{\rm front}$. Although our Figure 4 shows that $|v_F| \simeq (\alpha c_S)_{\rm front}$ in order of magnitude, our Figures 5, 10, and 12, which depict $|v_F|/(\alpha c_S)_{\rm front}$ in more detail, reveal a departure by up to a factor of $\sim$3 in $|v_F|/(\alpha c_S)_{\rm front}$ from unity. Anticipating future investigations of other systematic effects, we suspect that the scaling $|v_F| \simeq (\alpha c_S)_{\rm front}$ may hold to no better than a factor of $\lesssim$10 in regions with the strongest variations. MHS also mention finding a weak inverse relation between $|v_F|$ and $\alpha_{\rm cold}$, consistent with our results shown in Figure 12.

Our discussion of the relative importance of the different terms in the energy equation relates to the evolution of the disk during stagnation, which precedes the outburst in V. MHS discuss the physical effects and the relative importance of the different energy terms and show ratios of the

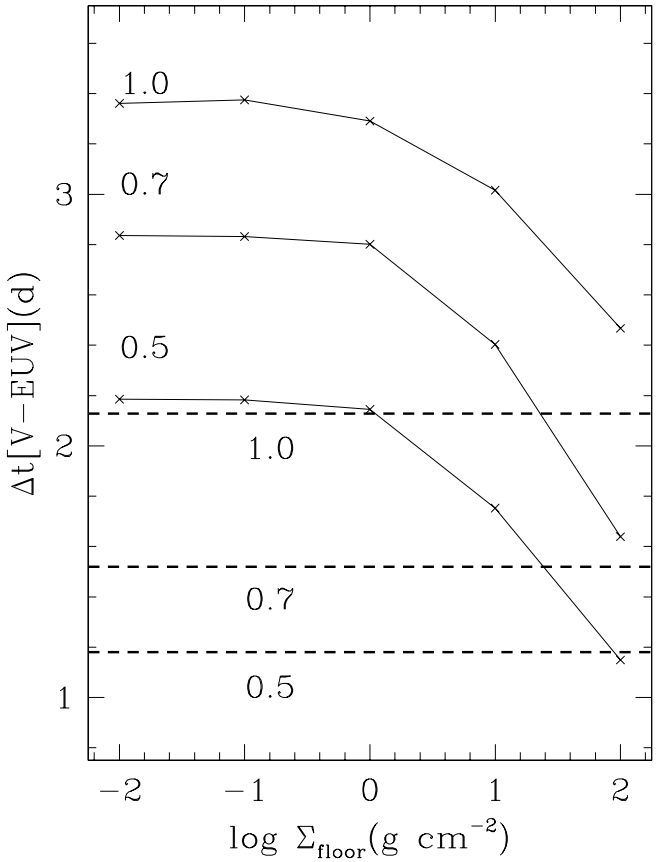

FIG. 9.—Delay times between the initial rapid rises in V and EUV fluxes for models in which the broad Σ distribution is not allowed to exceed a value $\Sigma_{\rm floor}$. The models adopt the SS Cyg parameters, and the numbers 0.5, 0.7, and 1.0 indicate the values of $r_{\rm instig}/r_{\rm disk}$. As $\Sigma_{\rm floor} \rightarrow 0$, the $\Delta t(V-{\rm EUV})$ value asymptotes to a constant which is about twice that found in our previous models (*dashed lines*).

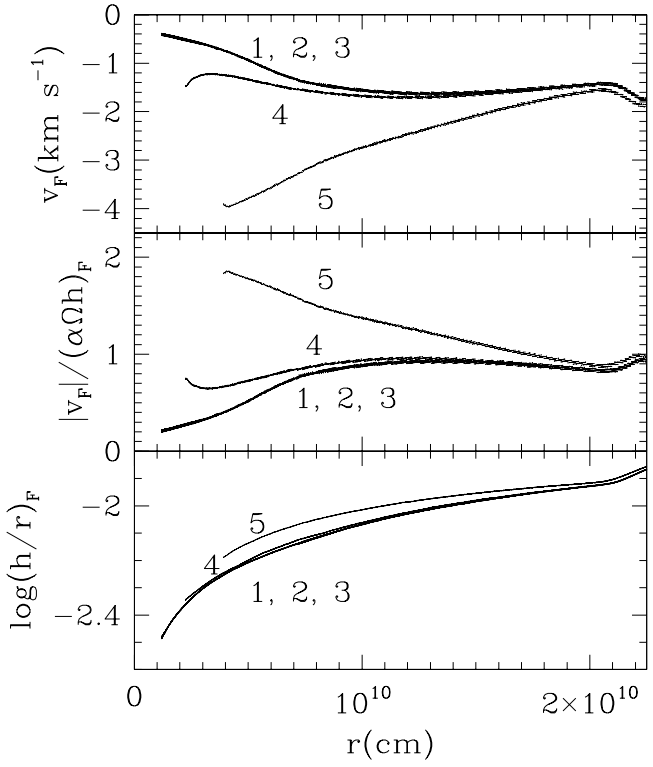

FIG. 10.—Heating front speeds and aspect ratios for the models shown in Fig. 9. The conventions are the same as in Fig. 5. The numbers 1, 2, 3, 4, and 5 denote $\Sigma_{\rm floor}$ values of 0.01, 0.1, 1, 10, and 100 g cm^{-2}, respectively.

terms to the heating term H at one time during the propagation of a heating front after stagnation has ended (see their Figs. 1 and 2). Since these times are different, we cannot directly compare our results to theirs. MHS show that, aside from a narrow precursor at the inner edge of the outside-in heating front, all terms except the cooling term C are negligible. All plots in MHS showing the ratios of the different energy terms to H are on a linear scale that allows one to see how H is small compared to the other terms within the narrow precursor on the leading edge of the heating fronts, but prevents one from assessing the relative ordering of the energy terms within the main body of the front, where the terms are of the order of, or smaller than, the heating term.

3. DISCUSSION

We have examined the delay between the onset of visual and EUV fluxes during a dwarf nova outburst, focusing on three systems for which complete V and EUV observations exist. We run 45 models spanning a range in systemic parameters, viscosity parameters, and triggering radii. When we combine our findings with those of Smak (1999), who prefers $\alpha_{\rm hot} = 0.2$ based on the normalization for the Bailey relation, we infer that the triggering radii must be close to the outer edge of the disk, at $\sim$0.6–0.7 of the primary's Roche radius. This seems consistent with the time-dependent calculations of Ichikawa & Osaki (1992)

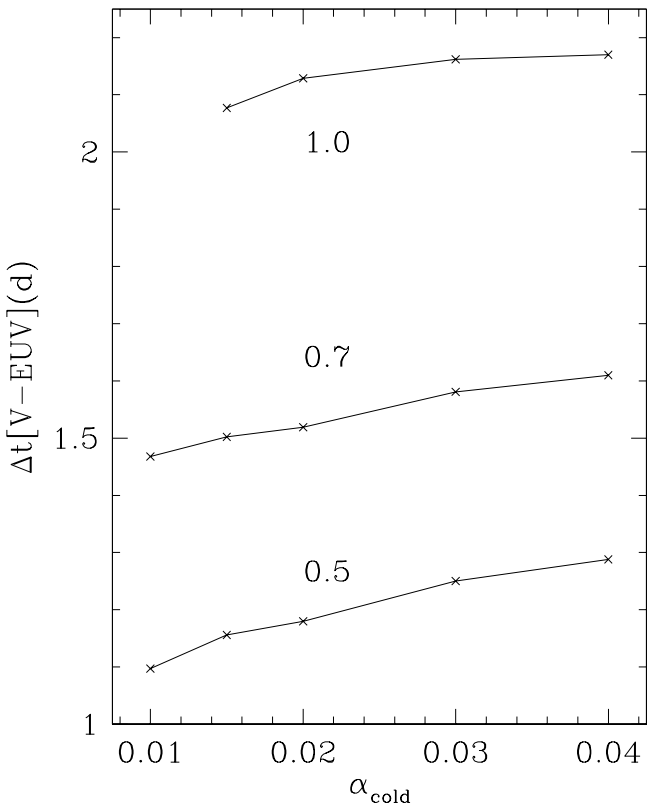

FIG. 11.—Delay times between the initial rapid rises in V and EUV fluxes as a function of $\alpha_{\rm cold}$. The models adopt the SS Cyg parameters, and the numbers 0.5, 0.7, and 1.0 indicate the values of $r_{\rm instig}/r_{\rm disk}$.

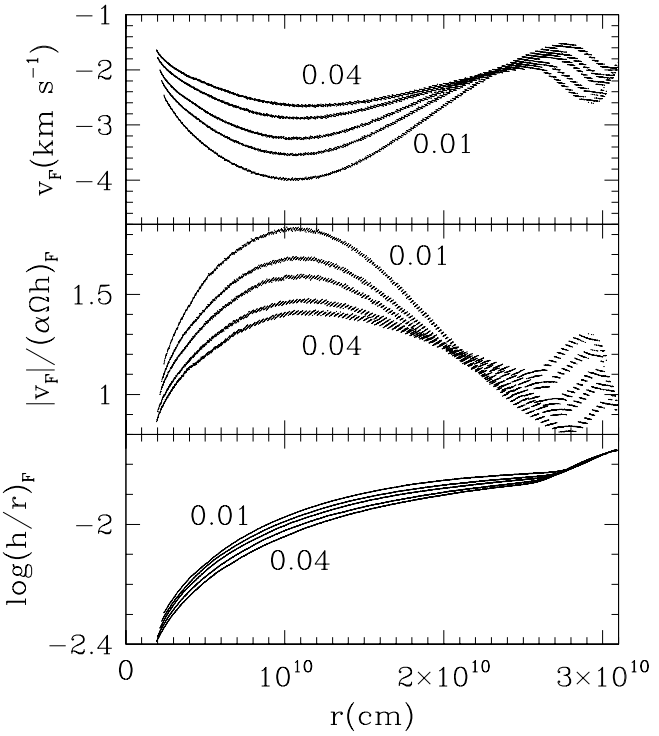

FIG. 12.—Heating front speeds and aspect ratios for the models shown in Fig. 11. The conventions are the same as in Figs. 5 and 10. The five curves in each panel represent $\alpha_{\rm cold} = 0.01, 0.015, 0.02, 0.03$, and 0.04.

and Smak (1998), which include a provision for a variable outer disk radius in which one sees a contraction of the outer disk in quiescence because of the accumulation of low angular momentum material from the secondary.

We see a prolonged period of stagnation after the thermal instability is triggered, during which time there is only a very gradual increase in the disk temperature and a slow spreading of the thermally unstable annulus. During stagnation one sees a weak maximum in Σ at the inner edge of the annulus that propagates to smaller radii. The speed of this front is also αc_S (where αc_S is evaluated at the peak of the spike), just as for the main heating front that begins later. It is slow because α and c_S are small. Stagnation lasts between $\sim$1 and 10 days in our simulations. Mineshige (1988) discusses several physical effects that contribute to stagnation. The only effect that appears not to be model dependent is that of the increased specific heat of gas at $\sim 10^4$ K because of the increased number of degrees of freedom of partially ionized gas. For instance, Mineshige discusses a contribution to stagnation due to the steep $T_{\rm eff}(\Sigma)$ dependence near the local maximum in Σ in the equilibrium $T_{\rm eff}(\Sigma)$ relation. This results in near equality between the heating and cooling functions during the early stages of the thermal instability. In this work we utilize three simple power-law scalings to describe the equilibrium $T_{\rm eff}(\Sigma)$ relation so as to remain as model independent as possible (C93b). Complications in the vertical structure due to physics that is not well understood, such as convection in a strongly sheared medium (Gu, Vishniac, & Cannizzo 2000), casts doubt on the trustworthiness of the detailed features of the equilibrium $T_{\rm eff}(\Sigma)$ relation, specifically the double hysteresis and intermediate stable branch of solutions that Mineshige (1988) uses in his calculations.

More generally, concerns raised by Gammie & Menou (1998) cast doubt on the standard assumption of having a well-defined $\alpha_{\rm cold}$ throughout quiescence. The lack of partial ionization may impede the operation of the MRI, which is thought to give rise to viscous dissipation and angular momentum transport in accretion disks. Fleming, Stone, & Hawley (2000) calculate the nonlinear saturation level of the MRI as a function of magnetic Reynolds number $\mathrm{Re}_M = c_S H/\eta$, where η is the resistivity, for a variety of assumptions concerning the initial magnetic field geometry. They find that there is no universal constant to which α saturates but rather there is a complicated model-dependent relation between Re_M and α (i.e., dependence on initial magnetic field configuration). Furthermore, it is unclear how strongly dependent the $\alpha(\mathrm{Re}_M)$ values found by Fleming et al. are on their specific computational model. There may also be other physical effects that need to be considered in the three-dimensional MHD calculations, such as Hall currents associated with the weakly ionized quiescent state, where large resistivity is an issue (Balbus & Terquem 2001). If MHD modelers of the MRI instability can reach a consensus on a general $\alpha(\mathrm{Re}_M)$ relation, that would serve as an impetus for time-dependent dwarf nova modelers to revisit their calculations.

Mineshige (1988) notes that the stagnation stage in his calculations lasts $\sim$1 day and states that stagnation lengthens the $V-$EUV delay more than in previous studies (PVW; CK). Mineshige suggests that the failure of the previous studies was tied to their oversimplified energy equation, specifically their adoption of a constant (and small) c_P value. This view is not borne out by our calculations. We find an abrupt increase in V by $\sim$5 mag lasting a few hours once stagnation has ended. Stagnation has no effect on the $V-$EUV delay: it only influences the evolution prior to the start of the rapid rise in V. (Indeed, were we to add the stagnation intervals of $\sim$1–10 days to the heating front travel times of $\sim$1–3 days, we would obtain delays considerably longer than observed. Mineshige might not have appreciated this since he only ran one model, for which the stagnation lasted $\sim$1 day.) There is a weak heating front associated with the spread of the warm region during stagnation, but the V flux is low during this entire phase. After stagnation has ended, a strong heating front forms, and 1–3 days later it reaches the WD. As noted by Smak (1998), the failure of earlier works was caused by their inability to produce outbursts that were triggered at sufficiently large radii. Although our results seem to contradict those of Mineshige (1988) by showing that stagnation has no effect on $\Delta t(V-\mathrm{EUV})$, it would probably be short-sighted on our part to assert that stagnation has no observational consequences. Various groups have claimed to see subtle changes in dwarf novae just prior to optical outburst (e.g., Mansperger & Kaitchuck 1990). Our simplified one-dimensional treatment of the disk equations and energy flow, coupled with our simplistic methods for computing the disk fluxes, do not currently allow us to make a firm theoretical prediction about the observational consequences of stagnation.

A contraction of the outer disk during quiescence, due to the accumulation of low angular momentum material and followed by an augmentation in the surface density at large radii, is one way to generate type A outbursts, but it is probably not the only way. Even within the context of the formalism for the treatment of the outer boundary condition introduced by Smak (1984) and based on earlier work

by Papaloizou & Pringle (1977), there are some apparent inconsistencies. For instance, Ichikawa & Osaki (1994) present a comparative study using both linear and nonlinear treatments of the tidal torque at large radii in the disk. They conclude that the expression utilized by Smak and later authors (e.g., Ichikawa & Osaki 1992; Hameury et al. 1998), in which the tidal torque varies as the fifth power of radius does not adequately represent the abrupt nature of the tidal cutoff at large radii (see Figs. 3 and 4 of Ichikawa & Osaki 1994). In addition, the strength of the tidal torque as characterized by its linear coefficient overpredicts the amplitude given by the full nonlinear calculation by about a factor of 20. Another consideration regarding type A versus type B outbursts is the work by Gammie & Menou (1998). They note that, as a result of the low partial ionization of the disk gas in quiescence, the MRI may be ineffectual, leading to a state of zero viscosity. This view is supported by Menou (2000), who finds runaway cooling during the transition to quiescence in a self-consistent model, using $\alpha(\mathrm{Re}_M)$ values from Fleming et al. (2000). If there were no other angular momentum transport mechanism operating in quiescence, the gas would pile up at some radius determined primarily by the specific angular momentum of the gas leaving the secondary star, and the triggering of the thermal instability might be the onset of some purely hydrodynamical instability within the accumulating torus. After interior temperatures rise to the point at which partial ionization is significant and the magnetic field entrained in the gas can couple effectively with the gas, the evolution would continue along the lines of what is presented in this paper. Alternatively, Menou (2000) suggests that some additional process such as spiral shocks may provide angular momentum transport and accretion during quiescence.

In accord with Meyer (1984) and Lin et al. (1985), we find the heating front speed is given (to within a factor of ~ 3) by $\alpha_{\mathrm{hot}} c_S$, where the sound speed c_S is evaluated within the heating front. This gives a delay time

$$\Delta t(V - EUV) = \int dr\, |\, v_F(r)\, |^{-1} \simeq 1.5 \text{ days} \left(\frac{r_s}{2.9 \times 10^{10} \text{ cm}}\right)^{1.5} \times \left(\frac{M_1}{1.2\ M_\odot}\right)^{-1/2} \left(\frac{\alpha_{\mathrm{hot}}}{0.2}\right)^{-1}, \quad (4)$$

where the input values have been scaled to those of SS Cyg and we assume $h/r = 0.01$ independent of radius. The "start" radius r_s is the point at which the strong heating front develops following stagnation; it is somewhat less than the instigation radius r_{instig} because of the slow spreading of the thermally unstable annulus during stagnation. This expression is general and should be applicable to other types of interacting binaries in which the accretion disk limit cycle operates, for instance the low-mass X-ray binaries in which the accreting object is a neutron star or black hole. Orosz et al. (1997) see a delay of ~ 6 days between the rise in V and soft X-ray flux during the onset of the 1996 April outburst in GRO J1655$-$40, a black hole candidate. Using our scaling for the delay and taking $M_1 = 6\ M_\odot$ gives $r_s = 1.3 \times 10^{11}$ cm, which is a considerable fraction of the outer disk radius expected, $\sim 4 \times 10^{11}$ cm, given the 2.6 day orbital period, i.e., enough to generate a type A outburst. This would indicate that the standard model can explain the delay for this system. Hameury et al. (1997) present an opposing view: they argue that the X-ray delay at outburst onset implies that a cavity must exist in the inner disk just prior to outburst so that the timescale to fill the inner disk is viscous rather than thermal, thereby reproducing the relatively long ~ 6 day delay. Our results fail to support this viewpoint: even if the inner disk were spreading into a vacuum, the front speed is still $\sim \alpha c_S$. Our Figure 9 shows that in the limit where $\Sigma_{\mathrm{floor}} \rightarrow 0$, the front travel time does not increase up to the viscous time $\sim (r/h)^2/\alpha\Omega$, but rather remains close to $\sim (r/h)/\alpha\Omega$.

For generality we have adopted the point of view that, while there is good theoretical and observational evidence for having a well-defined α_{hot} in the outburst state, the viscosity associated with quiescence is uncertain. This is unfortunate because the results presented herein show a significant dependence upon α_{cold}. If it does turn out to be the case that the viscosity in quiescence is nonlocal (e.g., proceeding via spiral shocks) or vanishingly small, however, the whole disk instability model for dwarf novae would have to be completely revised. This might then completely change the $V-$EUV delay times. For definiteness, we have had to work within the framework of the disk instability model, since that is the only quantitative model that currently exists. For full consistency, were one to argue that the current quiescent models are wrong and advocate an alternative (e.g., nonlocal angular momentum transport), the entire limit cycle model would then have to be revised based on the new assumptions. These comments also apply to the stagnation phase. Our results show that the stagnation phase is not detectable in the overall light curve. As mentioned earlier, this may depend on the simplified model that everyone currently uses, but in any event, the specific values of the stagnation times would be different in a drastically different model. Finally, in this paper we have dealt only with outside-in outbursts. Smak (1998) discusses and presents computations for inside-out outbursts as well.

4. CONCLUSION

We have presented a time-dependent parameter study of the onset of thermal instability for the accretion disks in dwarf novae, concentrating on parameters relevant to three well-studied systems: VW Hyi, U Gem, and SS Cyg. For each system, we look at the dependence of the delay between the initial rapid increase in V and EUV fluxes on triggering radii for the thermal instability within the disk and the α viscosity parameter for ionized gas. Our basic conclusion is that for $\alpha_{\mathrm{hot}} = 0.2$, inferred by Smak (1999) based on the Bailey relation for the decay of dwarf nova outbursts, we find that triggering must occur at large radii ~ 0.6–0.7 times the WD's Roche radius to produce delays that are as observed. We find that the speed of the inward-moving heating front that communicates the effect of the thermal instability is αc_S (evaluated within the heating front spike), in agreement with previous estimates. We also see a prolonged period (~ 1–10 days) of slow heating (stagnation) following the onset of thermal instability (Mineshige 1988). In contrast to Mineshige, we find that stagnation has no effect on the $V-$EUV delay since it precedes the rapid rise in V. In exploring the sensitivity of our results to the initial mass distribution, we find that as the background surface density is made smaller (i.e., all the mass is put into the torus at r_{instig} initially), the delay $\Delta t(V-\mathrm{EUV})$ increases by about a factor of 2 above that given by calculations in which the

background surface density $\Sigma_{\rm broad}$ initially is intermediate between the critical surface densities $\Sigma_{\rm min}$ and $\Sigma_{\rm max}$. For an upper limit background surface density $\Sigma_{\rm floor} \lesssim 1$ g cm^{-2}, the value of $\Delta t(V-{\rm EUV})$ is independent of $\Sigma_{\rm floor}$. If there were a significant amount of evaporation of the inner disk during quiescence, for instance, that depleted the $\Sigma(r)$ values interior to $r_{\rm instig}$ without changing $r_{\rm instig}$, this could increase $\Delta t(V-{\rm EUV})$ by up to a factor of ~ 2 above that found in other studies (e.g., Smak 1998). A logical next step would be to include some evaporation at a rate consistent with quiescent X-ray observations of dwarf novae into the time-dependent calculations of the limit cycle in order to quantify the effect of the depleted $\Sigma(r)$ distribution in the inner disk. It seems unlikely that a self-consistent inclusion of this effect would change $\Delta t(V-{\rm EUV})$ by as much as a factor of 2 given that the $\alpha_{\rm hot}$ values of ~ 0.2 inferred by Smak (1999) by independently fitting both the observed $\Delta t(V-{\rm EUV})$ values and rates of decay from outburst are in agreement. Finally, we find a weak inverse dependence of $\Delta t(V-{\rm EUV})$ on $\alpha_{\rm cold}$. This comes about because larger $\alpha_{\rm cold}$ values lead to smaller accretion disk masses (via the dependence of $\Sigma_{\rm max}$ on $\alpha_{\rm cold}$), so the heating front spike has a smaller amplitude and lower speed.

We thank Kimberly Engle, Damon Gunther, and David Friedlander in the Laboratory for High Energy Astrophysics at the NASA Goddard Space Flight Center for assistance in obtaining large amounts of CPU time on various workstations. We acknowledge useful discussions with Ethan Vishniac and John Hawley. We also thank the anonymous referee whose comments helped focus and improve the paper. Special thanks go to Chris Mauche whose detailed discussions and careful analysis and presentation of the dwarf nova data provided a strong impetus for carrying out this project.

REFERENCES

Anderson, N. 1988, ApJ, 325, 266
Bailey, J. 1975, J. Brit. Astron. Assoc., 86, 30
Balbus, S. A., & Hawley, J. F. 1991, ApJ, 376, 214
———. 1998, Rev. Mod. Phys., 70, 1
Balbus, S. A., & Terquem, C. 2001, ApJ, 552, 235
Buat-Meńard, V., Hameury, J.-M., & Lasota, J.-P. 2001, A&A, 366, 612
Cannizzo, J. K. 1993a, in Accretion Disks in Compact Stellar Systems, ed. J. C. Wheeler (Singapore: World Scientific), 6
———. 1993b, ApJ, 419, 318 (C93b)
———. 1994, ApJ, 435, 389
———. 1996, ApJ, 473, L41
———. 1998a, ApJ, 494, 366
———. 1998b, ApJ, 493, 426
———. 1998c, in ASP Conf. Ser. 137, Wild Stars in the Old West, ed. S. Howell, E. Kuulkers, & C. Woodward (San Francisco: ASP), 308
Cannizzo, J. K., Ghosh, P., & Wheeler, J. C. 1982, ApJ, 260, L83
Cannizzo, J. K., & Kenyon, S. J. 1987, ApJ, 320, 319
Cannizzo, J. K., & Wheeler, J. C. 1984, ApJS, 55, 367
Cannizzo, J. K., Wheeler, J. C., & Polidan, R. S. 1986, ApJ, 301, 634 (CWP)
Faulkner, J., Lin, D. N. C., & Papaloizou, J. 1983, MNRAS, 205, 359
Fleming, T. P., Stone, J. M., & Hawley, J. F. 2000, ApJ, 530, 464
Gammie, C. F., & Menou, K. 1998, ApJ, 492, L75
Gu, P.-G., Vishniac, E. T., & Cannizzo, J. K. 2000, ApJ, 534, 380
Hameury, J.-M., Lasota, J.-P., & Dubus, G. 1999, MNRAS, 303, 39
Hameury, J.-M., Lasota, J.-P., McClintock, J. E., & Narayan, R. 1997, ApJ, 489, 234
Hameury, J.-M., Menou, K., Dubus, G., Lasota, J.-P., & Huré, J.-M. 1998, MNRAS, 298, 1048
Hawley, J. F., & Balbus, S. A. 1991, ApJ, 376, 223
Ichikawa, S., & Osaki, Y. 1992, PASJ, 44, 15
———. 1994, PASJ, 46, 621
King, A. R. 1997, MNRAS, 288, L16
Lin, D. N. C., & Papaloizou, J. 1985, in Protostars and Planets II, ed. D. C. Black & M. S. Matthews (Tucson: Univ. Arizona Press), 981
Lin, D. N. C., Papaloizou, J., & Faulkner, J. 1985, MNRAS, 212, 105
Livio, M., & Pringle, J. E. 1992, MNRAS, 259, P23
Ludwig, K., & Meyer, F. 1998, A&A, 329, 559
Ludwig, K., Meyer-Hofmeister, E., & Ritter, H. 1994, A&A, 290, 473
Mansperger, C. S., & Kaitchuck, R. H. 1990, ApJ, 358, 268
Mauche, C. W., Mattei, J. A., & Bateson, F. M. 2001, Evolution of Binary and Multiple Stars, ed. P. Podsiadlowski, S. Rappaport, A. R. King, F. D'Antona, & L. Burderi (San Francisco: ASP), 367 (MMB)
Menou, K. 2000, Science, 288, 2022
Menou, K., Hameury, J.-M., & Stehle, R. 1999, MNRAS, 305, 79
Meyer, F. 1984, A&A, 131, 303
Meyer, F., & Meyer-Hofmeister, E. 1981, A&A, 104, L10
———. 1983, A&A, 128, 420
———. 1984, A&A, 132, 143
Mineshige, S. 1986, PASJ, 38, 831
———. 1988, A&A, 190, 72
Mineshige, S., & Osaki, Y. 1983, PASJ, 35, 377
———. 1985, PASJ, 37, 1
Mukai, K., Wood, J. H., Naylor, T., Schlegel, E. M., & Swank, J. H. 1997, ApJ, 475, 812
Orosz, J. A., Remillard, R. A., Bailyn, C. D., & McClintock, J. E. 1997, ApJ, 478, L83
Osaki, Y. 1996, PASP, 108, 39
Papaloizou, J., Faulkner, J., & Lin, D. N. C. 1983, MNRAS, 205, 487
Papaloizou, J., & Pringle, J. E. 1977, MNRAS, 181, 441
Pratt, G. W., Hassall, B. J. M., Naylor, T., Wood, J. H., & Patterson, J. 1999, MNRAS, 309, 847
Pringle, J. E., Verbunt, F., & Wade, R. A. 1986, MNRAS, 221, 169
Ritter, H., & Kolb, U. 1998, A&AS, 129, 83
Schreiber, M. R., Gänsicke, B. T., & Hessman, F. V. 2000, A&A, 358, 221
Shakura, N. I., & Sunyaev, R. A. 1973, A&A, 24, 337
Smak, J. 1984, Acta Astron., 34, 161
———. 1998, Acta Astron., 48, 677
———. 1999, Acta Astron., 49, 391
Stehle, R., & King, A. R. 1999, MNRAS, 304, 698
Truss, M. R., Murray, J. R., Wynn, G. A., & Edgar, R. G. 2000, MNRAS, 319, 467
van Teeseling, A. 1997, A&A, 319, L25
Warner, B. 1987, MNRAS, 227, 23
———. 1995, Cataclysmic Variable Stars (Cambridge: Cambridge Univ. Press)